On the effective friction law of a heterogeneous fault

Michel Campillo and Pascal Favreau[1]
Laboratoire de Géophysique Interne, Observatoire de Grenoble, Université Joseph Fourier
Grenoble, France

Ioan R. Ionescu
Laboratoire de Mathématiques, Université de Savoie, Campus Scientifique
Le Bourget-du-Lac, France

Christophe Voisin[2]
Laboratoire de Géophysique Interne, Observatoire de Grenoble, Université Joseph Fourier
Grenoble, France

Abstract. Numerical simulation of the rupture process is usually performed under an assumption of scale invariance of the friction process although heterogeneous fault properties are shown by both direct observations of surface crack geometry and slip inversion results. We investigate if it is possible to define an effective friction law for a finite fault with a small-scale heterogeneity, that is, with a distribution of narrow segments with a resistance to rupture higher than the rest of the fault. We consider a model where the local boundary condition corresponds to a linear slip-dependent friction law. We define the effective slip-dependent friction law by analogy with the theoretical spectral solution for the initiation phase in the case of a homogeneous infinite fault. We use finite difference simulations to test the validity of this approach. The results show a surprisingly good agreement between the calculations for the complete heterogeneous fault model and for a homogeneous fault with an effective friction law. The time of initiation and the average of the slip velocity on the fault are well predicted by the effective model. The effective friction law exhibits a nonlinear slip dependence with an initial weakening rate different from the one of the local laws. This initial weakening rate is related to the geometry of the heterogeneity and can be obtained by an eigenvalue analysis. The effective law shows a kink at a slip that corresponds to the average slip on the fault for which the stress concentration of the strong segments is sufficient to trigger their rupture. While based on a rather simple model of a fault, these results indicate that an effective friction can be defined and used for practical purposes. The heterogeneity of a fault tends to decrease the initial weakening rate of the local weak patches. Since the initial weakening rate controls the initiation duration, this last point indicates that the duration of initiation expected from actual heterogeneous faults is much larger than the one deduced from small-scale laboratory measurements. The actual fracture energy is not conservative in the rescaling of the friction law.

1. Introduction

Friction is a phenomenon that concerns both microscopic and macroscopic scales. The origin of friction has to be found in the hard contacts between two rough surfaces. The phenomenon is observed in seismology at the scale of the seismic waves, that is kilometric. Hence the fault heterogeneity described by the inversion of seismological data by *Hartzell and Heaton* [1983], *Archuleta* [1984], and *Cotton and Campillo* [1995] is also of kilometric scale. The smallest scales of heterogeneity cannot be obtained directly. Even the laboratory measurements [*Dieterich*, 1979; *Ohnaka and Shen*, 1999] do not represent the local boundary condition at the microscopic scale but the macroscopic frictional behavior of the elastic bodies in contact at the scale of the samples. The geometry of the contact, let us say the roughness,

[1]Now at Institute for Crustal Studies, University of California, Santa Barbara, California.
[2]Now at Dept. of Geological Sciences, San Diego State University, San Diego, California.
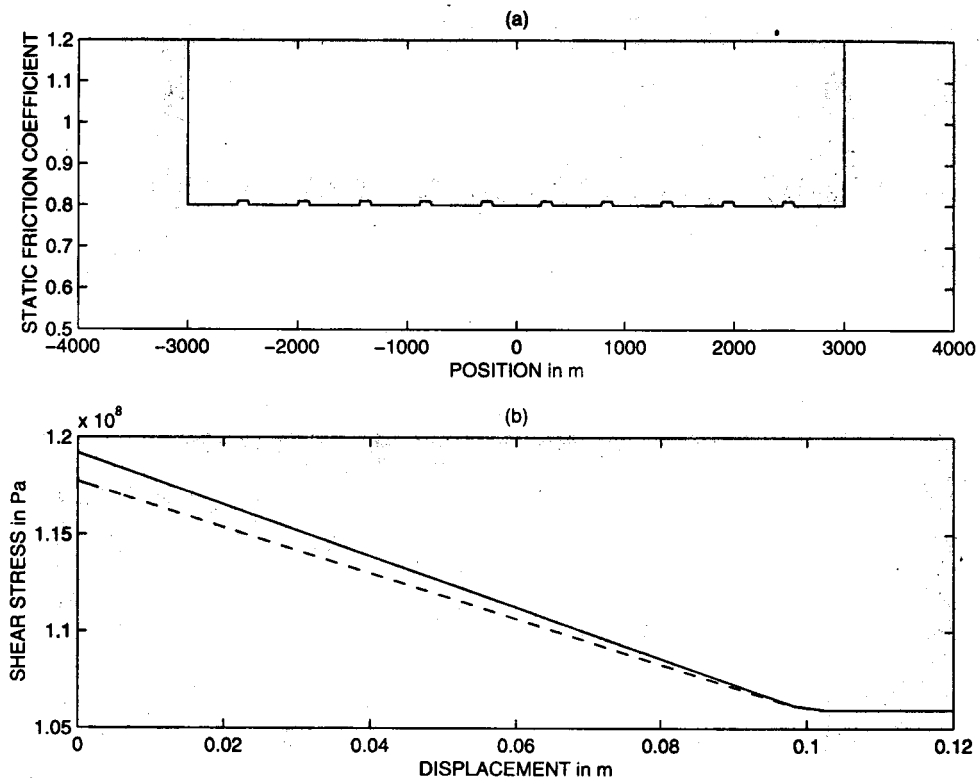
Figure 1. (a) Static friction coefficient on the fault. The extremities are assumed to be unbreakable. (b) The friction law on the strong (solid line) and weak (dashed line) patches.

has been shown to be a decisive parameter for frictional behavior [*Scholz*, 1990]. The contact can be modeled at different scales as a nonlinear process resulting in a friction law. Models of a macroscopic slip-dependent friction law have been proposed from the analysis of the microscopic physical behavior of a rough surface of contact [see *Matsu'ura et al.*, 1992]. In the classical approach of the nonlinear problem of slipping with weakening, the scale invariance is implicitly assumed for crack theory [*Andrews*, 1976; *Madariaga*, 1976; *Fukuyama and Madariaga*, 1998]. In these theories the same effective friction law is assumed for every time scale or space scale. The aim of this paper is to investigate this assumption using simple numerical experiments. We aim to check the assumption that there exists an equivalent macroscopic friction law for the problem of a fault with small scale strength heterogeneity. By equivalent, we mean that this "macroscopic" effective law is sufficient to describe the global behavior of the fault.

Our analysis concerns primarily the initiation phase which is an unstable and highly dynamic stage of rupture. This stage corresponds to the evolution of the friction from its static level to its dynamic value. It is therefore the best stage to describe the friction evolution. Indeed, the friction law governs also the rupture propagation and one of our objectives is to test the accuracy of an effective friction law in the description of the complete process. We performed numerical experiments based on the finite difference method described by *Ionescu and Campillo* [1999]. The present paper concentrates on a single change of scale from the point of view of classical mechanics. We expect that this type of approach can provide useful information about the rules of scaling that can be included in more general conceptual models of earthquake behavior such as those based on simplified interaction between elementary patches [*Burridge and Knopoff*, 1967; *Carlson and Langer*, 1989] or based on a hierarchical approach [*Narteau et al.*, 2000].

2. Heterogeneous and Equivalent Problems

The macroscopic behavior of a fault with small-scale heterogeneity of rupture resistance is difficult to relate to the local properties of the fault. Since the friction law appears as a local boundary condition, the local (microscopic) properties are kept fixed in the global process. A formal measure of the friction on the fault itself would just be a local particular law, that is varying with the position along the fault. In this paper we focus on the following question: How can we obtain an effective (equivalent) friction law which, used on a homogeneous fault, leads to a slip evolution similar to the one produced on the heterogeneous fault?

We now present the heterogeneous and equivalent homogeneous problems. In the following, we shall denote with the indexes h and e the fields, equations, laws, etc., attached to the heterogeneous and equivalent problem, respectively. If no index is used, it means that the field or equation is the same for both problems.
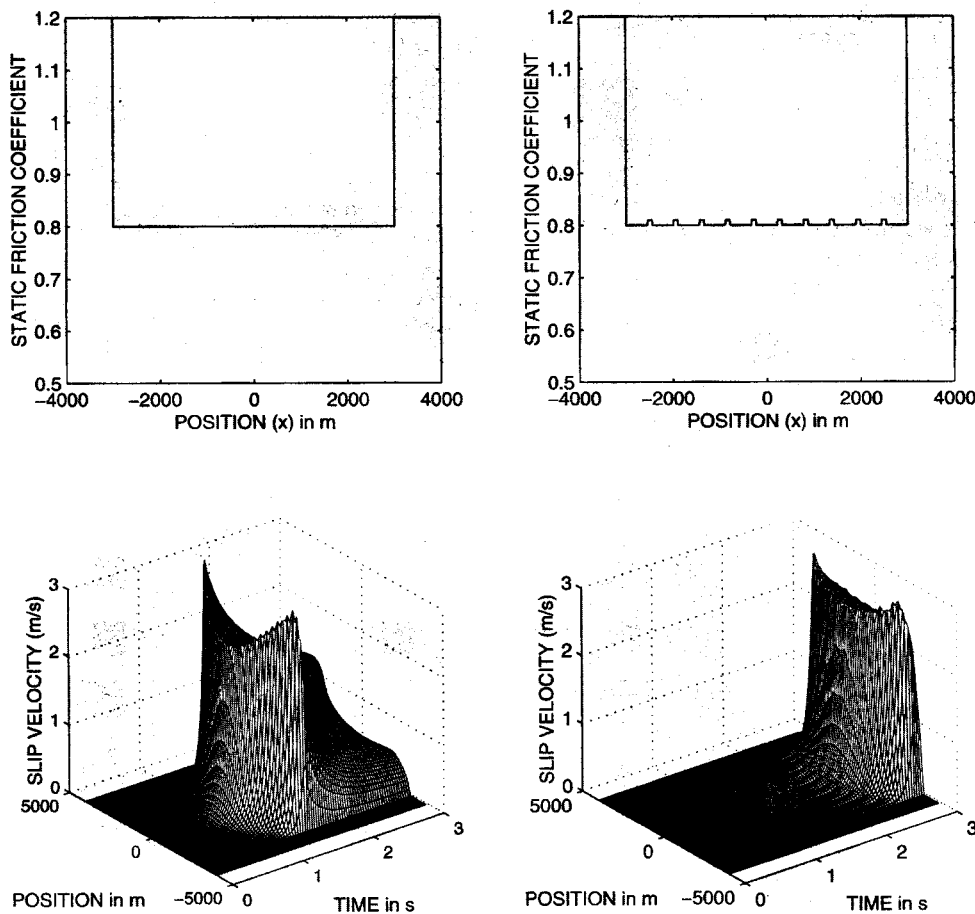
Figure 2. Comparison between the initiation on (left) a homogeneous and (right) an inhomogeneous finite fault. The distribution of strength is presented on top of the evolution of slip velocity on the fault.

We consider the antiplane shearing on a finite fault $y = 0$, $|x| < a$ of length $2a$, denoted by Γ_f, limited by unbreakable barriers, in a homogeneous linear-elastic space. The contact on the fault is described by a slip-dependent friction law. We assume that the displacement field (u_x, u_y, u_z) is 0 in directions Ox and Oy and that u_z does not depend on z. The displacement u_z is therefore denoted simply by $w(t, x, y)$. The elastic medium has the shear rigidity G, the density ρ and the shear velocity $c = \sqrt{G/\rho}$. The nonvanishing shear stress components are $\sigma_{zx} = \tau_x^\infty + G\partial_x w(t, x, y)$ and $\sigma_{zy} = \tau_y^\infty + G\partial_y w(t, x, y)$, and the normal stress on the fault plane is $\sigma_{yy} = -S$ ($S > 0$, that is the compression stress is negative).

The equation of motion is

$$\frac{\partial^2 w}{\partial t^2}(t, x, y) = c^2 \nabla^2 w(t, x, y), \qquad (1)$$

for $t > 0$ and (x, y) outside of the fault Γ_f.

Concerning the boundary conditions on Γ_f, we have

$$\sigma_{zy}(t, x, 0^+) = \sigma_{zy}(t, x, 0^-), \quad |x| < a, \qquad (2)$$

and the friction law. For the heterogeneous problem, the slip-dependent friction law is

$$\sigma_{zy}^h(t, x, 0) = \mu^h(x, \delta w^h(t, x))S, \quad \partial_t \delta w^h(t, x) > 0, \quad (3)$$

$$\sigma_{zy}^h(t, x, 0) \leq \mu^h(x, \delta w^h(t, x))S, \quad \partial_t \delta w^h(t, x) = 0, \quad (4)$$

for all $|x| < a$, where $\delta w^h(t, x) = 1/2\ [w^h(t, x, 0^+) - w^h(t, x, 0^-)]$ is the half of the relative slip and $\mu^h(x, \delta w)$ is the coefficient of friction on the heterogeneous fault which will be described below. We consider here a series of strong patches of width b which are evenly distributed on the fault (see Figure 1a). They form a surface of strong resistance Γ_f^s with a large static friction coefficient $\mu_s^s = \mu^h(x, 0)$ if $x \in \Gamma_f^s$. The other part of the fault, denoted Γ_f^w, has a weak static resistance $\mu_s^w = \mu^h(x, 0)$ if $x \in \Gamma_f^w$. It is composed of a series of weak patches of width b_w. We call $\delta\mu_s = \mu_s^s - \mu_s^w > 0$ the increase of static resistance on the barriers. Everywhere on the fault we assume a linear slip-weakening friction. The dynamic friction μ_d and the critical slip L_c are assumed constant on the fault. In conclusion, the heterogeneous friction coefficient $\mu^h(x, \delta w)$ is a piecewise linear function illustrated in Figure 1b and given by

$$\mu^h(x, \delta w) = \mu_s^s - \frac{\mu_s^s - \mu_d}{L_c}\delta w, \quad x \in \Gamma_f^s, \qquad (5)$$

$$\mu^h(x, \delta w) = \mu_s^w - \frac{\mu_s^w - \mu_d}{L_c}\delta w, \qquad x \in \Gamma_f^w, \quad (6)$$

for all $\delta w \le L_c$ and

$$\mu^h(x, \delta w) = \mu_d, \qquad \delta w > L_c, \ |x| < a. \quad (7)$$

To simplify our analysis, we consider here the same dynamic friction μ_d on the weak and strong fault.

On the equivalent fault we shall consider a homogeneous friction law (i.e., μ is not dependent on the position x on the fault):

$$\sigma_{zy}^e(t, x, 0) = \mu^e(\delta w^e(t, x))S, \quad \partial_t \delta w^e(t, x) > 0, \quad (8)$$

$$\sigma_{zy}^e(t, x, 0) \le \mu^e(\delta w^e(t, x))S, \quad \partial_t \delta w^e(t, x) = 0, \quad (9)$$

for all $|x| < a$, where $\delta w^e(t, x) = 1/2 \ [w^e(t, x, 0^+) - w^e(t, x, 0^-)]$ is the half of the relative slip and $\mu^e(\delta w)$ is the coefficient of friction on the equivalent (homogeneous) fault. Note that for the equivalent problem we will not assume a linear slipweakening. Indeed, because of the progressive breaking of the barriers, the slip-weakening properties of the heterogeneous fault are changing during the process. As a consequence, we expect that the slipweakening of the effective fault have to change resulting in a nonlinear slip-weakening law. Since in the case considered here, the dynamic friction coefficient is homogenous on the heterogenous fault, the effective friction law will eventually exibit the same coefficient when the weakening phase is finished everywhere.

The initial conditions are denoted by w_0 and w_1, that is,

$$w(0, x, y) = w_0(x, y), \quad \frac{\partial w}{\partial t}(0, x, y) = w_1(x, y). \quad (10)$$

Since our intention is to study the evolution of the elastic system near an unstable equilibrium position, we shall suppose that $\tau_y^\infty = S\mu_s^w$ is the static value of the friction force on the weak part of the heterogeneous fault. We remark that taking w as a constant satisfies (1)-(4); hence $w \equiv 0$ is a metastable equilibrium position, and w_0, w_1 may be considered as small perturbation of the equilibrium.

Finally, let us state the main goal of this paper: Find the equivalent friction law $\mu^e(\delta w)$ such that the equivalent displacement field $w^e(t, x, y)$ is a good approximation for the heterogenous displacement field $w^h(t, x, y)$ obtained with a heterogenous friction law $\mu^h(x, \delta w)$ during the initiation and propagation stages.

3. A Simple Heterogeneous Fault Model

We consider a fault of finite length $2a$ with $a = 3000$ m as presented in Figure 1 and described in the previous Section 2. Note that this length can be scaled with respect to the friction parameters [Dascalu et al., 2000]. A discussion of this scaling appears further in this section. The dynamic friction is assumed homogeneous on the fault. The instability begins with a small

perturbation of velocity at the center of the fault and the process is modeled with a finite difference scheme [Ionescu and Campillo, 1999]. We consider a medium with a density $\rho = 3000$ kg.m^{-3} and a shear velocity $c_s = 3000$ m.s^{-1}. The friction law parameter for the weak patches are $\mu_s^w = 0.8$, $\mu_d = 0.72$ and $L_c = 0.1$m. The normal stress corresponds to a depth of 5000 m and its value is $S = 1.4715 \times 10^8$ Pa. These parameters of the models are kept constant all over the paper.

In the first model we consider the presence of 11 weak patches of width $b_w = 455$ m separated by 10 strong patches of width $b = 100$ m corresponding to an increase of strength $\delta\mu_s = 0.01$ so that $\mu_s^s = 0.81$. While modest, this heterogeneity has a considerable influence on the development of the shear instability. This is illustrated in Figure 2. We compare the results obtained with and without the presence of the strong patches using the same friction law. In the case of an homogeneous fault the instability develops rapidly and the slip velocity profiles have smooth shapes. These features have been described by Campillo and Ionescu [1997] in the infinite case and by Dascalu et al. [2000] for finite faults. In presence of strength heterogeneity the slip velocity profiles display small irregularities that are indeed characteristic of the distribution of the strong patches. Furthermore, the instability development is much slower than for a homogeneous fault with $\mu_s = 0.8$. Our goal here is to check if the behavior of the heterogeneous fault can be reproduced by using a model of homogeneous fault with an "effective" friction law. Let us first discuss the conditions of this numerical experiment with respect to the theoretical stability analysis of Dascalu et al., 2000. In the case of the homogeneous (weak) fault, i.e., $\delta\mu_s = 0$ in our case, they introduced a nondimensional weakening parameter β defined by

$$\beta = a\alpha_c, \qquad \alpha_c = \frac{S(\mu_s - \mu_d)}{GL_c}. \quad (11)$$

Dascalu et al. [2000] found that when β is larger than a critical value $\beta_0 = 1.15774$, the instability can occur. With the parameters used here $\beta = 13.08$ (i.e., much larger than the critical value β_0 which limits the stability domain of the system) the homogeneous weak fault behaves like an infinite fault during the initiation. Let consider now the case of an isolated weak patch of the heterogeneous model. The value of β in this case is $b_w S(\mu_s^w - \mu_d)/(2GL_c) = 0.981$ that is less than β_0. That means that such a weak patch is not long enough to allow the instability to develop with the friction law considered here. However as shown in Figure 2, the instability develops on a series of weak patches separated by narrow zones of resistance because of the elastic interaction between the slipping patches. This interaction is difficult to represent mathematically but one can easily figure out the process by considering a simple analogy. The presence of a series of weak patches lowers the apparent stiffness of the body and therefore leads to a

broader domain of instability than for a single isolated slipping patch.

4. Dynamic Evaluation of the Effective Friction Law

To obtain an effective friction law for the heterogeneous fault, in this section, we rely on theoretical results obtained for the initiation of an infinite homogeneous fault. It is possible to extrapolate this results to the case of a finite fault when it is large enough that its finiteness has no influence on the initiation process, that is when the nondimensional parameter β is much larger than $\beta_0 = 1.1577....$(as it was discussed in Section 3). For the infinite homogeneous fault, *Campillo and Ionescu* [1997] used a spectral method to separate the complete displacement $w^e(t,x,y)$ into a "wave part" that corresponds to propagation of the initial perturbation and a "dominant part" $w_d^e(t,x,y)$ that describes the exponential time growth of the instability. Rapidly, the wave part becomes negligible and the solution can be identified to the dominant part, i.e.,

$$w^e(t,x,y) \approx w_d^e(t,x,y), \qquad (12)$$

which has the form

$$w_d^e(t,x,y) = \frac{\alpha_c}{\pi}\exp(-\alpha_c y)\{\int_{-\alpha_c}^{\alpha_c}\int_0^\infty\int_{-\infty}^\infty$$

$$\exp(-\alpha_c s + i\alpha(x-u))[\text{ch}(ct\sqrt{\alpha_c^2 - \alpha^2})w_0(u,s)$$

$$+ \frac{\text{sh}(ct\sqrt{\alpha_c^2 - \alpha^2})}{c\sqrt{\alpha_c^2 - \alpha^2}}w_1(u,s)]dudsd\alpha\}, \qquad (13)$$

with

$$\alpha_c = -\frac{\mu' S}{G}, \qquad (14)$$

where

$$\mu' = \frac{\partial \mu}{\partial \delta}. \qquad (15)$$

Equation (13) shows an important property of the displacement field inside the volume during the initiation process: the evolution of the displacement along y is simply described by $\exp(-\alpha_c y)$. This is an almost obvious consequence of the condition of slip-dependent friction that can be obtained by any linearization around the equilibrium. In the very simple conditions considered so far, it is an important property since it indicates that a parameter of the local boundary condition on the fault (the rate of slip weakening $G\alpha_c$) can be retrieved directly from the knowledge of the displacement field in the bulk. The shear stress in the bulk $\sigma_{zy}^e(t,x,y)$ can be approximated by $G\partial_y w^e(t,x,y)$, and therefore, during the initiation, the derivative of strain with respect to displacement, that is, $-\frac{1}{G}\frac{\partial \sigma_{zy}^e(t,x,y)}{\partial w_d^e(t,x,y)}$ is equal to $-\alpha_c$. Alternatively, we note that $-\frac{1}{S}\frac{\partial \sigma_{zy}^e(t,x,y)}{\partial w_d^e(t,x,y)}$ gives the rate of slip weakening μ' on the fault. There is no

spatial scale involved in the infinite problem. Nevertheless, this shows that the local friction characteristics on the fault are governing the displacement field in an extended region around the fault. In this homogeneous case the local property on the fault (at the microscopic scale) is the same as the one inferred in the elastic bulk (at the macroscopic scale). Indeed, this reasoning is strictly valid in the domain of application of the linearization used by *Campillo and Ionescu* [1997]. When the slip reaches L_c, the crack propagation begins on a part of the fault and the problem becomes heterogeneous. At the same time the stress on the fault remains constant and we can expect that at a point in the bulk close to the fault, the stress remains constant too. The stress-displacement relation in the bulk therefore mimics perfectly the friction on the fault, and we verify it numerically. For the infinite fault we saw that α_c can be obtained by computing the derivative of strain with respect to displacement. In the following, when more general configurations are considered, we will refer to this derivative as

$$\gamma(t,x,y) = \frac{-1}{G}\frac{\partial \sigma_{zy}^e(t,x,y)}{\partial w_d^e(t,x,y)}. \qquad (16)$$

Let us now apply the ideas presented for the infinite problem to the case of a finite homogeneous fault. We concentrate on the initial weakening. Figure 3 presents the displacement field a short time after the initial perturbation. At the time considered (0.23 s), the process is still in the initiation stage as it can be seen on Figure 2. The processing of this displacement field leads to a map of the parameter $\gamma(t,x,y)$, the derivative of shear strain with respect to displacement, that corresponded to α_c in the theory of the infinite fault. This parameter was computed for every point where the displacement is larger than a threshold value of 10^{-6} m. One must note the narrow range of values used in the representation in Figure 3. It is remarkable that the value of γ measured in the vicinity of the fault is precisely the expected value for the weakening law considered here (4.36×10^{-3} m^{-1}). This computation shows that knowing the displacement field outside the fault, one could retrieve the weakening on the fault, even in the case of a finite fault when, as here, the fault length is much larger than the slipping patch. Indeed, for a homogeneous fault, it was just a formal exercise and a numerical validation.

We can now study in the same way the case of a heterogeneous fault such as that considered for the computation presented in Figure 2. We shall use the numerical experiments to check if the property of the homogeneous problem can be applied to a problem with a heterogeneity of small scale. Our goal here is to define a nonlocal effective friction law that can be used to renormalize the problem with a small-scale heterogeneity into an homogeneous one. So far, there is no evidence that an effective friction law could be defined for an heterogeneous fault.
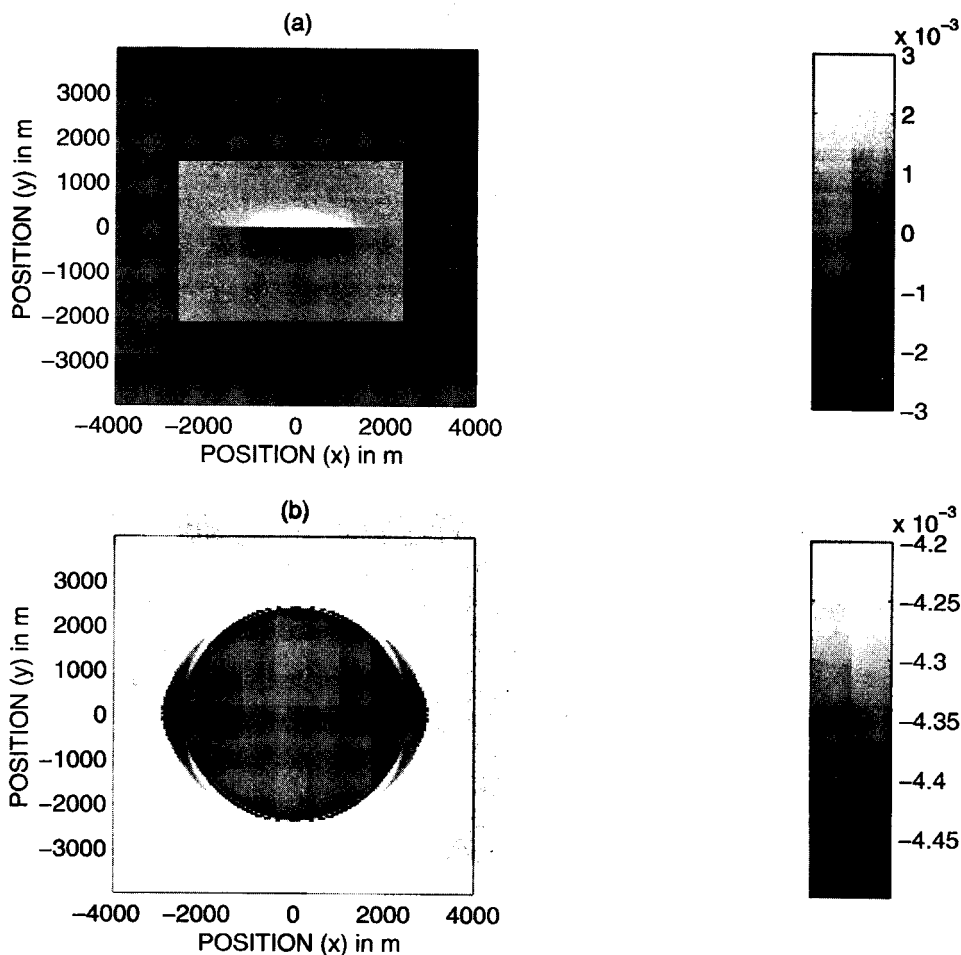
Figure 3. (top) Displacement at a time $t = 0.23$ s during the initiation as a function of x and y. The computation corresponds to the one presented in Figure 2. (bottom) Derivative of strain with respect to displacement, parameter γ, as a function of x and y at the same time. The value of α_c associated with the friction law in the infinite fault theory is 4.36×10^{-3} m^{-1}.

5. Definition of the Effective Friction Law and Test of Its Accuracy

We rely directly on the analogy with the homogeneous problem to define an effective or renormalized friction law. Using the numerical results of the heterogeneous fault model corresponding to Figure 3, we measure in the bulk the relation between the stress and the slip for the initiation phase, that is, before the arrival of the waves associated with the propagation of crack fronts on the different sections of the fault. To choose the point of measure, let us examine the distribution of displacement and strain. We consider first a time near the beginning of the initiation phase. Figure 4 presents the results obtained in a similar manner as was performed in Figure 3 for the homogeneous finite fault. At this point the barriers still resist, and the initiation occurs only on the weak patches. The heterogeneity of the displacement field is clearly visible on Figure 4 (top). Indeed, this heterogeneity is also present on the distribution of the derivative of strain with respect to displacement. Nevertheless, in spite of the narrow range of values used in the plot it is remarkable to notice that

at a distance from the fault larger than the width of the weak patches, an almost constant value of γ is reached. This indicates the emergence of a simple collective behavior that will be interpreted as an eigenmode in section 6. Note that close to the initial wave front (causality limit), one can observe a criss-cross pattern which corresponds to the initial conditions that had been imposed to start the instability. As it will be discussed in section 6, the problem remains formally unchanged as long as the barriers are resisting. It is interesting to visualize what happens when the barriers fail. When the first barrier begins to break, the initiation process accelerates, and very rapidly all of the barriers are broken. The resistance of the fault is strongly affected, and we expect a large apparent weakening rate. This can be visualized by looking at the γ parameter during this transition as it is illustrated in Figure 5. Note that in this case the plotting scale is much larger than in Figures 3 and 4. At a time of 2.4 s, the barriers are still resisting; γ has a value of 1.63×10^{-3} m^{-1} in a broad region around the fault. The slip begins at the barriers at the center of the fault at 2.57 s. At 2.73 s, γ reaches a much larger value in the region around the
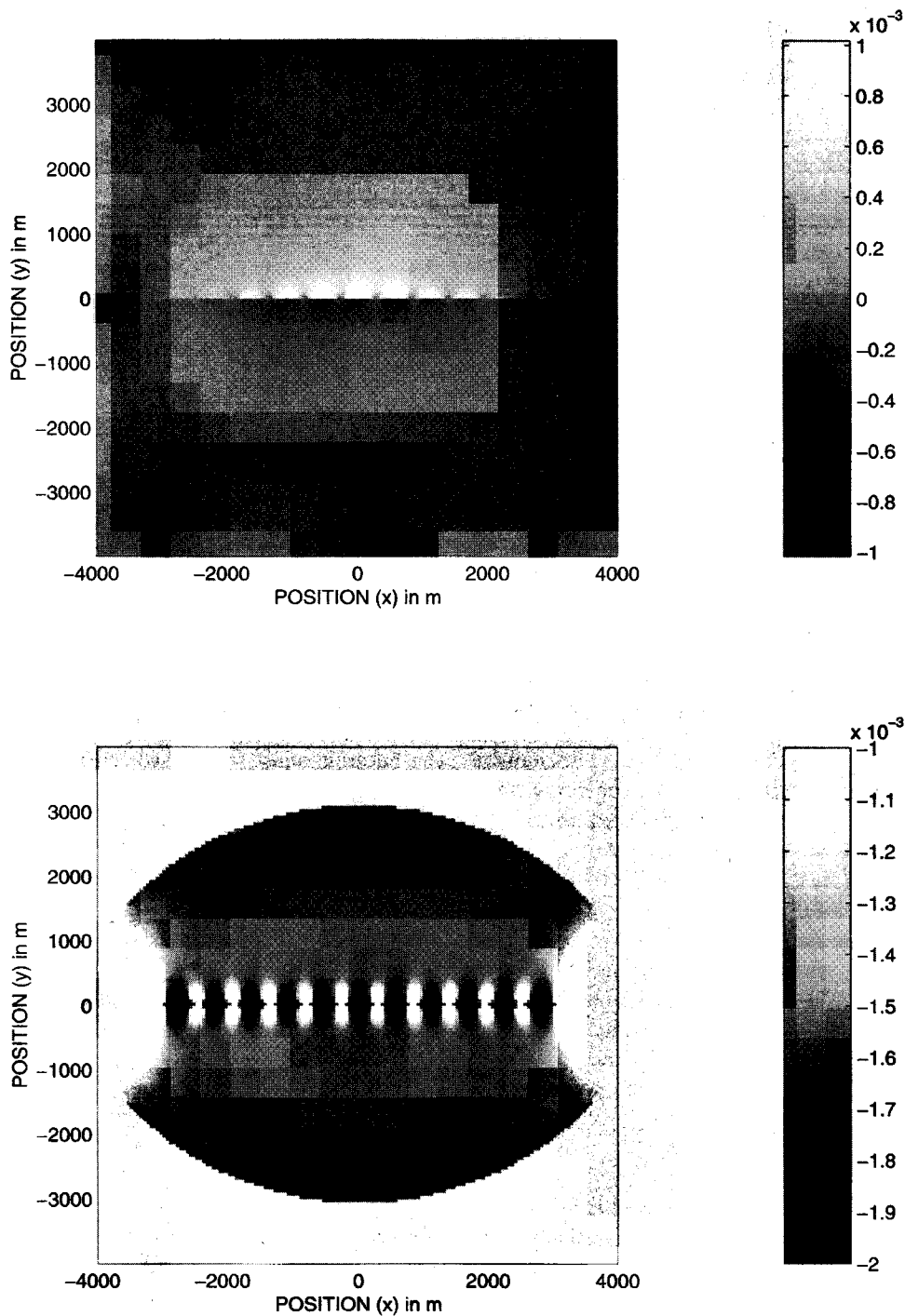
Figure 4. (top) Displacement at a time t=0.27s during the initiation, as a function of x and y for the heterogeneous fault. The computation corresponds to the one presented in Figure 2. (bottom) Derivative of strain with respect to displacement (γ) as a function of x and y at the same time. Note the constant value of γ in a broad region around the fault.

slipping strong patches, indicating a strong apparent weakening. Soon after, at 2.9 s, the entire central part of the fault has slipped more than L_c, and the stress on the fault is constant and equal to the dynamic friction. The corresponding apparent weakening is therefore null as shown in Figure 5. Again this can be observed in the elastic bulk. The three stages of the physical evolution of the fault are well marked in the values of γ. This suggests that the effective friction can be found in the bulk at a distance from the fault of the order of
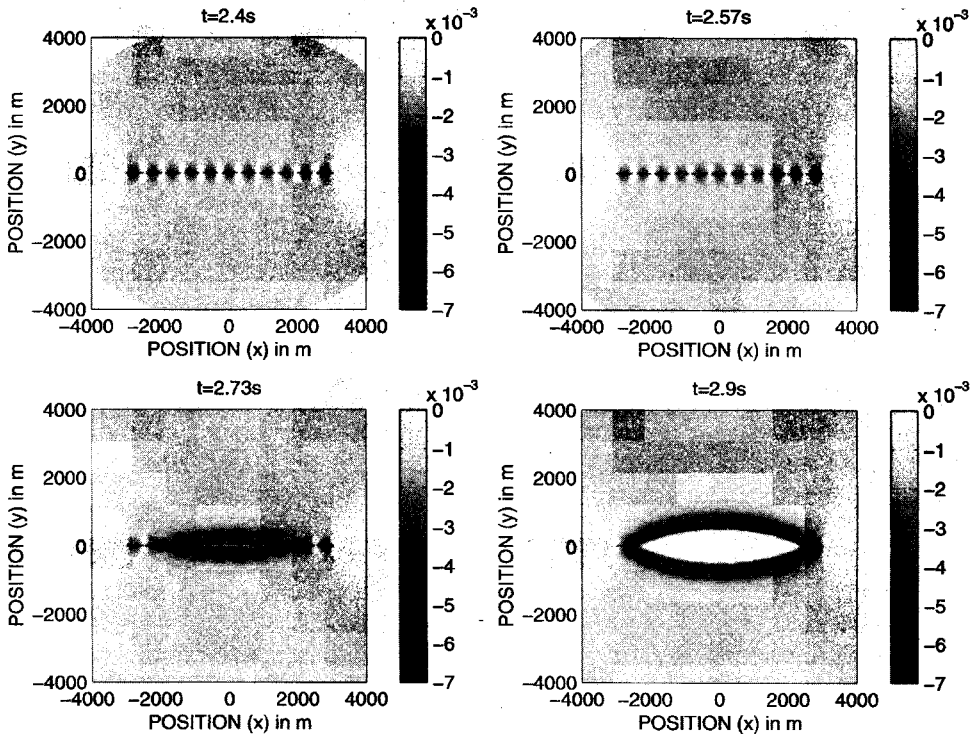
Figure 5. (top) The γ parameter at the end of the initiation process and at the beginning of rupture propagation. Note the change of γ with time at a given point.

the distance between two strong patches. This can be expected since the elastic properties of the body have an averaging effect on the displacement field associated with the boundary friction conditions. We can check the accuracy of this rather naive approach by a numerical test. In Figure 6 we present the stress-displacement relation that we propose to use as an effective friction law. It is directly derived from the numerical test at a point: $x = 1000$ m measured from the center of the fault and $y = 400$ m away from the fault. We use it directly as the local condition on the surface of an homogeneous fault with the same length. Figure 6 shows a comparison between the slip velocity profiles on the fault at different times for the complete heterogeneous model and for the homogeneous one with the effective friction law. The global agreement is excellent. Indeed, the homogeneous model cannot account for the details of the profile in the heterogeneous case, but the timing of the growth of the instability and the average shape of the velocity profile at every times are perfectly reproduced. The results presented in Figure 5 suggest that the agreement extents further the domain of initiation in the one of crack propagation. Part of the success of this comparison can be understood by considering the existence of a global mode of growth of the instability on the fault as it will be explained in the section 6. One can note on Figure 6 that the weakening rate of the effective law at the origin is smaller than the one of the reference fault. As discussed by *Ionescu and Campillo* [1999], this weakening rate governs the duration of the initiation. The increase of duration of initiation due to

the heterogeneity (as illustrated in Figure 2) is directly expressed in the effective law by the smaller initial weakening rate (Figure 6, middle).

In order to investigate the domain of applicability of this approach, we performed a series of tests with increasing $\delta\mu_s$. In Figure 7 we present a comparison between the heterogeneous model and the effective one for $\delta\mu_s = 0.05$. As already stated, an homogeneous model cannot account for the peculiarities of an heterogeneous one, as the high frequency wave radiation for example. Nevertheless we find again an excellent agreement concerning the timing of the instability evolution and the smoothed shape of the velocity profiles. This numerical expriment shows that the renormalization can be performed for a broad range of models and leads to useful results for the simulation. We performed a series of computations to test the sensitivity of our results to the numerical conditions. We verified carefully that our results are independent of the grid size. To do so, we considered a grid 2 times, then 8 times smaller, and we obtained almost indistinguishable effective friction laws. We tested also the dependence of the effective law on the position and shape of the initial perturbation. Again, the test showed the robustness of the evaluation of the effective law. In section 6, we enter into further details of the theoretical justification of our technique.

6. Spectral Evaluation of the Effective Friction Law

The spectral analysis relies on a linearization method, valid in the initiation phase when the stress evolves from
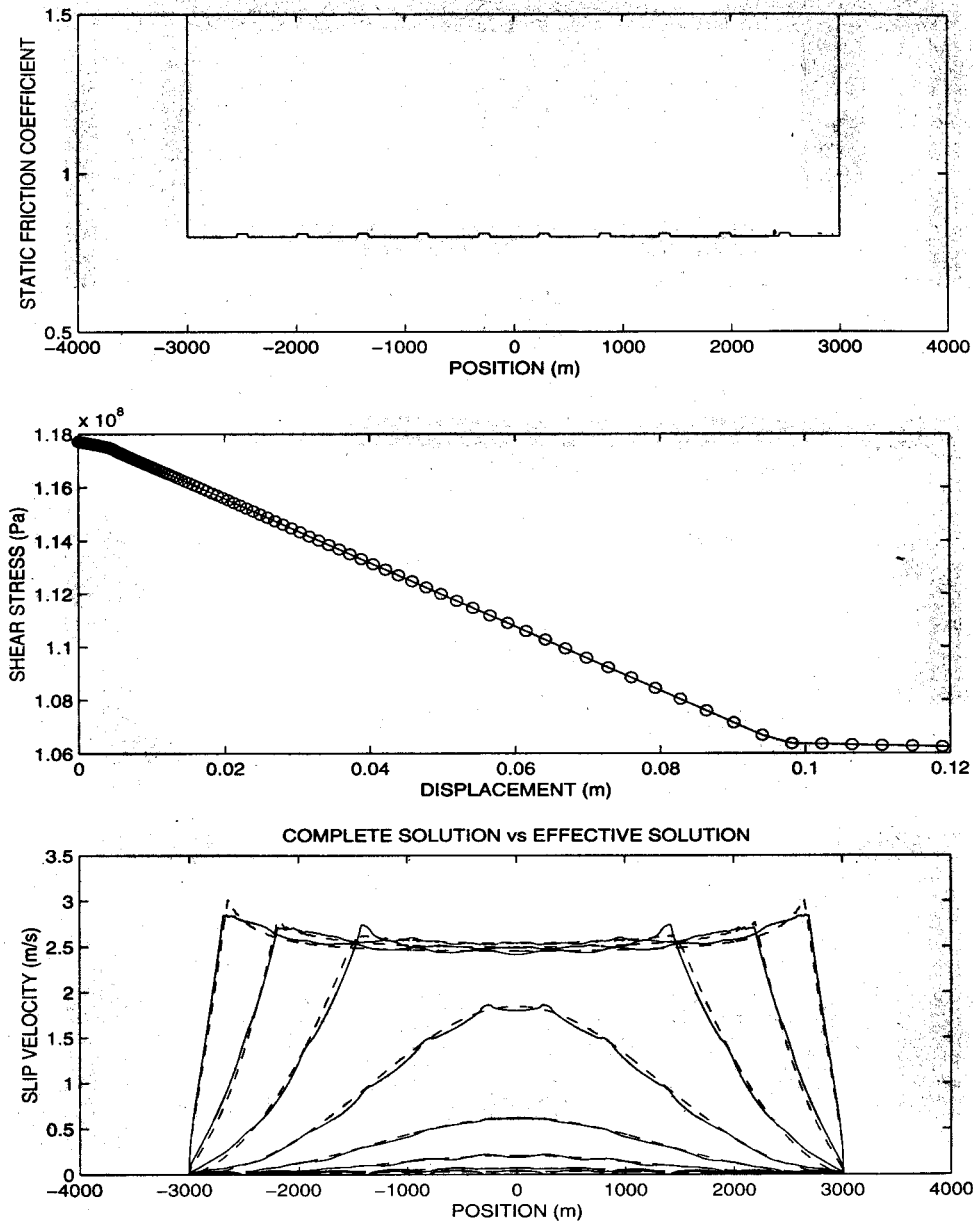
Figure 6. (top) Profile of static resistance along the fault. (middle) Effective friction law used in the computation. (bottom) Comparison between the complete solution (solid line) and the results obtained with the effective friction law (dashed lines) at the same times.

the fault strength to the dynamic stress. Indeed, it is a peculiarity of the law with constant weakening rate used here. *Campillo and Ionescu* [1997] used a spectral method to solve the problem of the initiation of shear instability on a homogeneous infinite fault. In the case of an unstable finite fault with homogeneous friction properties, the initiation develops according to a finite set of eigenfunctions associated with positive eigenvalues that govern the exponential evolution of the instability. The process evolution is dominated by the greatest positive eigenvalue λ_0^2. Indeed the displacement can be generically written in its spectral expansion as

$$w(t,x,y) = \sum_{i=0}^{\infty}[\mathrm{ch}(ct\lambda_i)W_0^i + \mathrm{sh}(ct\lambda_i)W_1^i]\Phi_i(x,y),$$
$$(17)$$

where $\lambda_0^2 > \lambda_1^2 > \dots$ are the eigenvalues (which are real and satisfy $\lim_{i\to\infty} \lambda_i^2 = -\infty$) and Φ_i are the corresponding eigenfunctions. After a period of time the term which involves $\exp(ct\lambda_0)$ completely dominates all other terms in the series, hence we can write

$$w(t,x,y) \approx [\mathrm{ch}(ct\lambda_0)W_0^0 + \mathrm{sh}(ct\lambda_0)W_1^0]\Phi_0(x,y). \quad (18)$$

To obtain an effective friction law for the heterogeneous fault, we rely on theoretical results obtained for the initiation of an homogeneous fault. Indeed, we shall define the effective or equivalent friction as the slip-dependent function which generates the same first positive eigenvalue as the one associated with the heterogeneous problem. As we have seen in section 5, the effective laws can be reasonably approximated by piecewise linear functions (Figures 6 and 7). The two different
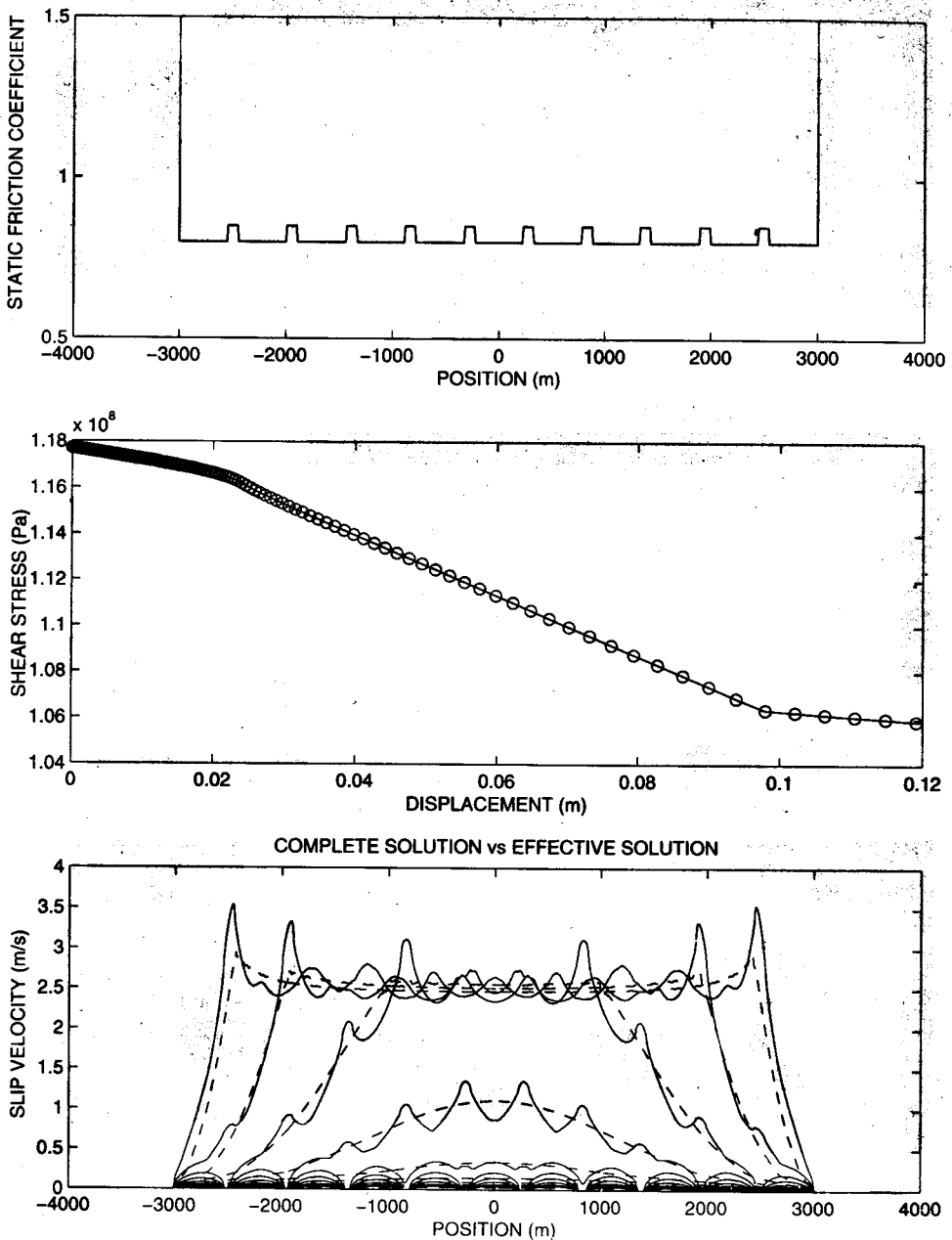
Figure 7. (top) Profile of static resistance along the fault. Center: Effective friction law used in the computation. (bottom) Comparison between the complete solution (solid line) and the results obtained with the effective friction law (dashed lines) at the same times.

slopes shown on these figures correspond to only two different successive eigenvalues in the initiation on the heterogeneous fault. They define two periods which we shall refer to as early and final initiation.

The spectral analysis is based on a linearization of the heterogeneous problem. The early initiation corresponds to a linear slip-weakening friction on the weak part of the heterogeneous fault while the barriers remain intact. This linearization is valid until the beginning of slip on one asperity that defines the end of the early initiation stage.

Formally, at the beginning of the instability (i.e., in the early initiation) in the heterogeneous model considered here, the problem can be linearized in the form

of an eigenvalue problem: find the heterogeneous early initiation eigenfunction Φ_e^h and eigenvalue $(\lambda_e^h)^2$ such that

$$\nabla^2 \Phi_e^h(x,y) = (\lambda_e^h)^2 \Phi_e^h(x,y), \qquad y > 0, \quad (19)$$

$$\Phi_e^h(x,0) = 0, \qquad |x| > a \text{ or } x \in \Gamma_f^s, \quad (20)$$

$$\frac{\partial}{\partial y}\Phi_e^h(x,0) = -\alpha_w^h \Phi_e^h(x,0), \qquad x \in \Gamma_f^w, \quad (21)$$

where α_w^h is a parameter which has the dimension of a wave number (m^{-1}) given by

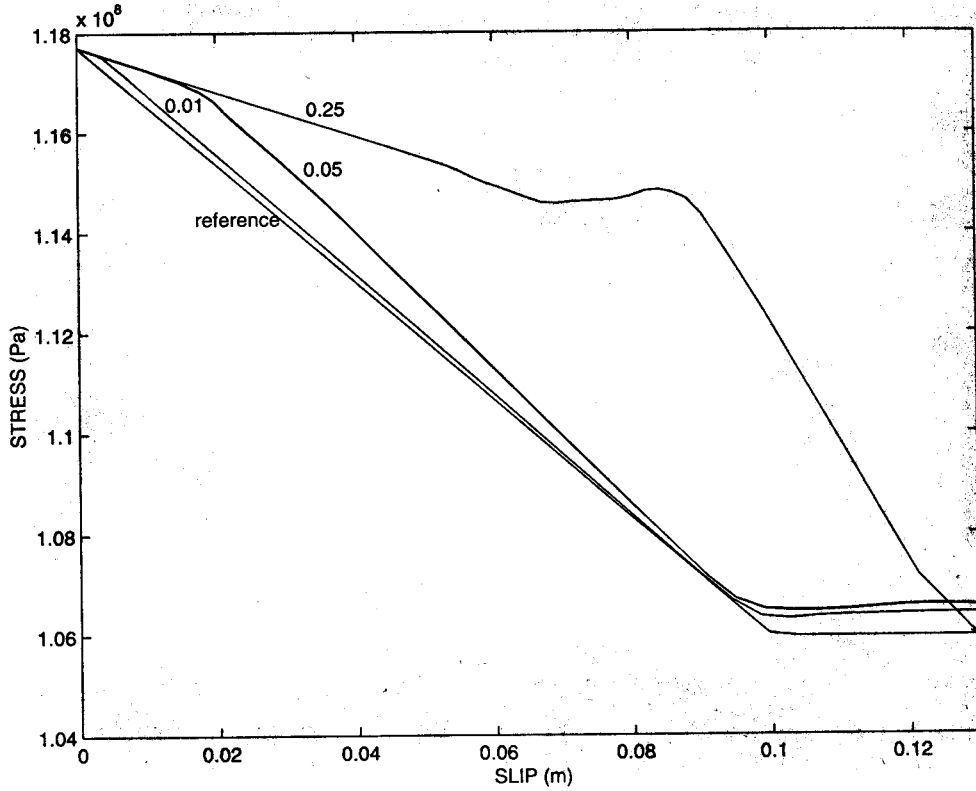$$\alpha_w^h = \frac{(\mu_s^w - \mu_d)S}{GL_c}. \quad (22)$$

Figure 8. The stress-displacement relations measured in the bulk for different heterogeneous models. The values of $\delta\mu$ are indicated. The local friction law is also shown as reference.

Since we deal with a symmetric operator we have real-valued eigenvalues $(\lambda_e^h)^2$, i.e., λ_e^h is real or purely imaginary. This type of problem requires a numerical resolution. It can be achieved quite easily using a finite element method (C. Voisin et al., Spectral analysis of the initiation process on a bounded fault region, submitted to *Geophysical Journal International*, 2000, hereafter referred to a Voisin et al., submitted manuscript, 2000). Let us denote by λ_{e0}^h, the greatest real eigenvalue (we suppose that it exits) and the associated eigenfunction Φ_{e0}^h of (19)-(21).

Let us consider now the spectral problem of the homogeneous case associated with the early initiation stage: Find the effective early initiation eigenfunction Φ_e^e and eigenvalue $(\lambda_e^e)^2$ such that

$$\nabla^2\Phi_e^e(x,y) = (\lambda^e)^2\Phi_e^e(x,y), \qquad y > 0, \quad (23)$$

$$\Phi_e^e(x,0) = 0, \quad |x| > a, \qquad (24)$$

$$\frac{\partial}{\partial y}\Phi_e^e(x,0) = -\alpha\Phi_e^e(x,0), \qquad |x| < a. \quad (25)$$

Let us denote by $\lambda_0^e = \Lambda(\alpha)$, the greatest real eigenvalue of (23)-(25). This spectral problem was already studied by *Dascalu et al.* [2000] with an integral method and Voisin et al. (submitted manuscript, 2000) using a finite element method. They computed the relation between the first eigenvalue λ_0^e and the wave number α. From the function Λ we can deduce the early initiation equivalent wave number α^e and the corresponding weakening

rate $\mu_e' = -G\alpha_e^e/S$ for the effective model. Indeed, α_e^e is deduced such that we have the same eigenvalue as in the heterogeneous case, i.e., $\Lambda(\alpha_e^e) = \lambda_{e0}^h$ which gives

$$\mu_e' = -\frac{G}{S}\Lambda^{-1}(\lambda_{e0}^h). \qquad (26)$$

For large values $b_w\alpha_w^h >> \beta_0 = 1.1577...$, i.e., large λ_e^h or "rapid" initiation, we know that the infinite fault solution can approximate the initiation phase on a finite fault [see *Ionescu and Campillo*, 1999]. Hence we can use the analytical (and not numerical) simple formula for $\lambda_{e0}^e(\alpha)$ obtained by *Campillo and Ionescu* [1997] in the case of an infinite fault, i.e.,

$$\Lambda(\alpha) \approx \alpha. \qquad (27)$$

In this way we can deduce the approximative formula for effective weakening rate in the early initiation:

$$\mu_e' \approx -\frac{G}{S}\lambda_{e0}^h. \qquad (28)$$

As soon as the asperities begin to break, the linearization above loses its validity. There is then a complex phase with a completely nonlinear, heterogeneous problem. Our numerical experiments indicate that once a barrier begins to slip, its neighbors slip very soon after. The change of behavior is very rapid in the cases we studied. When all the barriers are slipping, the problem again reduces to a linear problem. The linear slip dependence of the friction has two different slopes on the
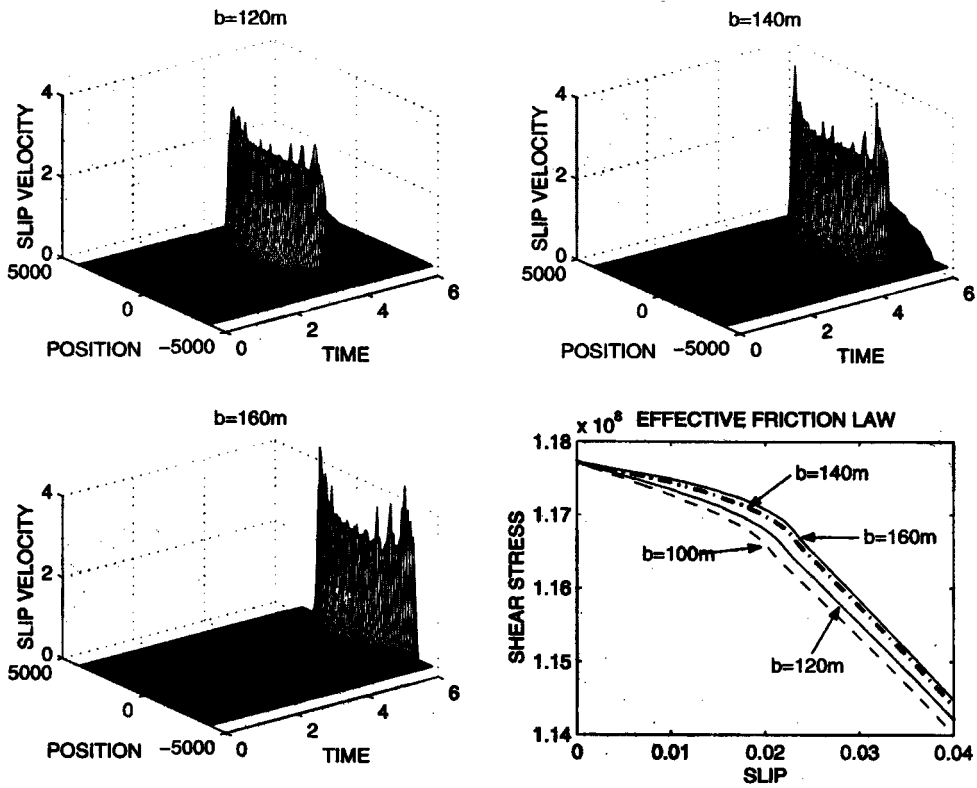
Figure 9. Slip velocity as a function of space and time for different values of b, the width of the barrier asperities. The corresponding effective friction laws are plotted at the same scale.

heterogeneous fault corresponding to the weak or strong parts. We shall call this stage the final initiation. We have first considered the early stage of initiation. Let us find now the weakening rate of the effective friction law during the final initiation stage. For this we will consider the heterogeneous eigenvalue problem corresponding to the period when all the barriers are slipping, i.e., find the heterogeneous final initiation eigenfunction Φ_f^h and eigenvalue $(\lambda_f^h)^2$ such that

$$\nabla^2 \Phi_f^h(x,y) = (\lambda_f^h)^2 \Phi_f^h(x,y), \qquad y > 0, \quad (29)$$

$$\Phi_f^h(x,0) = 0, \qquad |x| > a, \qquad\qquad (30)$$

$$\frac{\partial}{\partial y}\Phi_f^h(x,0) = -\alpha_w^h \Phi_f^h(x,0), \qquad x \in \Gamma_f^w, \quad (31)$$

$$\frac{\partial}{\partial y}\Phi_f^h(x,0) = -\alpha_s^h \Phi_f^h(x,0), \qquad x \in \Gamma_f^s. \quad (32)$$

where α_s^h is a wave number corresponding to strong patch and given by

$$\alpha_s^h = \frac{(\mu_s^s - \mu_d)S}{GL_c}. \qquad (33)$$

Let us denote by λ_{f0}^h, the greatest real eigenvalue (we suppose that it exists) and the associated eigenfunction Φ_{f0}^h of (29)-(32). We can deduce now the final initiation wave number α_f^e and the corresponding weakening rate $\mu_f' = -G\alpha_f^e/S$ for the effective model such that we have the same eigenvalue as in the heterogeneous case, i.e., $\Lambda(\alpha_f^e) = \lambda_{f0}^h$ which gives

$$\mu_f' = -\frac{G}{S}\Lambda^{-1}(\lambda_{f0}^h). \qquad (34)$$

As in the early initiation stage, for large values of $a\alpha_w^h >> \beta_0 = 1.1577...$, i.e., large λ_f^h, we have the approximative formula (27) for effective weakening rate during the final initiation stage:

$$\mu_f' \approx -\frac{G}{S}\lambda_{f0}^h. \qquad (35)$$

We performed numerical computations of eigenvalues using the finite element approach of Voisin et al. (submitted manuscript, 2000). Both homogeneous and heterogeneous fault were considered, and we found a good agreement between the weakening rates presented in Figures 6 and 7 and the effective ones deduced from the eigenvalue analysis. For example, for the early initiation, which leads to the same results for the two cases presented, we found an effective weakening rate $\mu_e' = 0.299$ m^{-1} from the results of the finite difference computation while we obtain a value $\mu_e' = 0.287$ m^{-1} from the eigenvalue analysis.

7. Influence of the Amplitude of the Friction Heterogeneity

We present in Figure 8 the effective friction laws corresponding to the reference homogeneous case, to the two heterogeneous cases previously considered, and to an heterogeneous model with $\delta\mu_s = 0.25$. This last
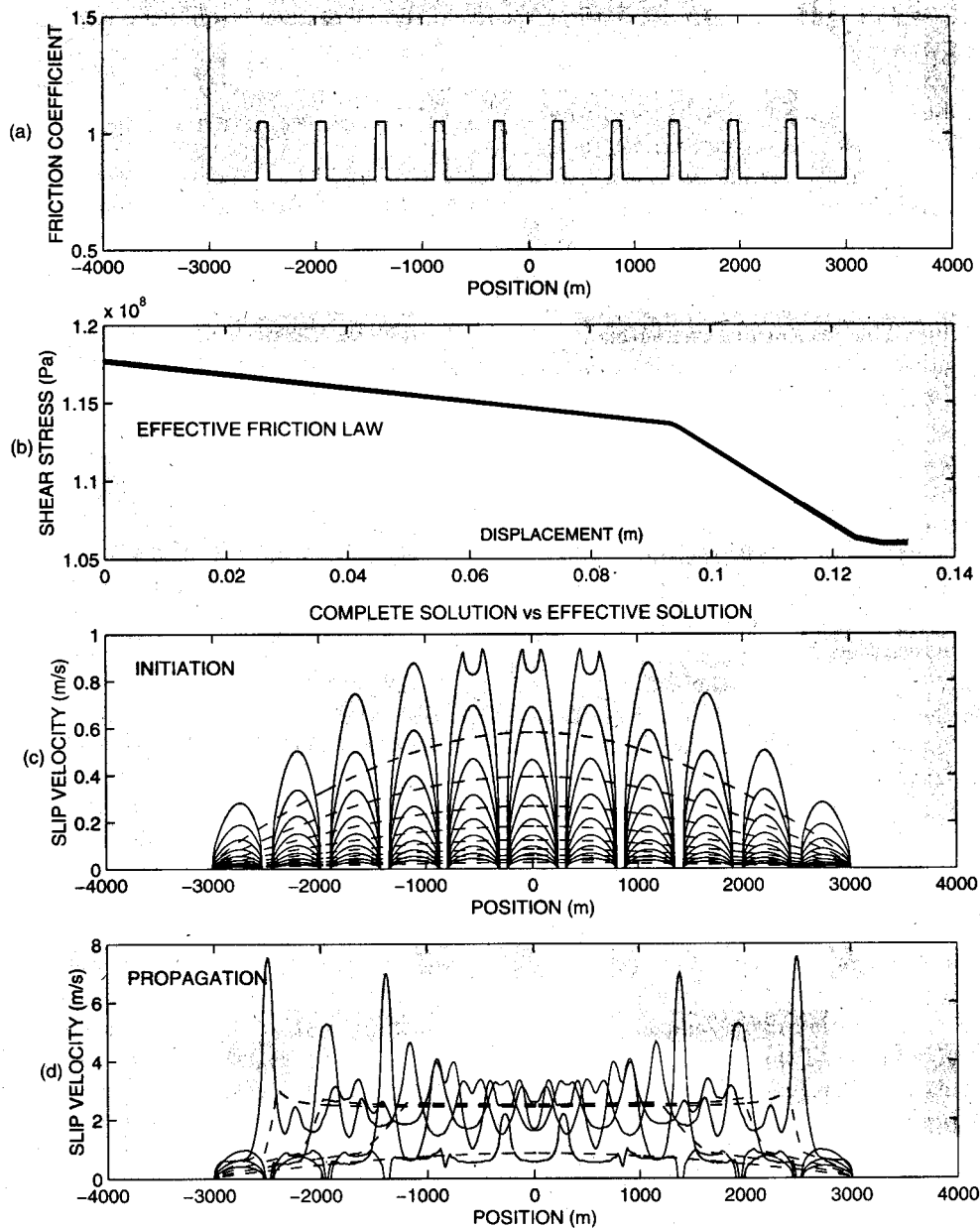
Figure 10. (top) Profile of static resistance along the fault. (middle) Effective friction law used in the computation. (bottom) Comparison between the complete solution (continuous line) and the results obtained with the effective friction law (dashed lines) at the same times. The comparison is presented in the initiation and propagation phases in two separated subplots.

value represents a very strong heterogeneity for which the resistance on the strong patches exceeds the normal stress. Figure 8 shows simple properties of the effective friction law. The most obvious observation is that the rate of weakening at the origin is the same for the three models, that is, independent of the amplitude of the perturbation. This weakening is governed by the geometry of the distribution of heterogeneities, which is the same for the three models. Physically, the instability experiences the same resistance until the static threshold on the strong patches is reached. The apparent weakening at the beginning is therefore in all cases the same as for a series of faults separated by unbreakable barriers. In other words, this weakening is directly linked to

the first eigenvalue of the problem of the initiation on a series of finite faults. The weakening rate changes when the stress concentration on the strong patches reaches the static resistance. The weakening rate is then intermediate between those of the weak and strong patches. One can verify that the slip at the change in slope is roughly proportional to $\delta\mu_s$, as expected from a simple model of stress concentration at a crack tip. In the case of $\delta\mu_s = 0.25$ the stress-displacement relation in the bulk for the initiation phase is perturbed by the strong emission of waves produced by the rupture of the strong patches. We shall show in section 8 that it is nevertheless possible to extract an effective law from this curve.

8. Influence of the Geometry of the Heterogeneity

Since the instability develops at first through the interaction between weak patches, we can expect that the strong patch width is an important parameter which controls the initial weakening rate of the effective friction law. In order to visualize the effect of this parameter, we performed a series of computations with the different values of b: $120, 140$ and 160 m and a constant value of $\delta\mu_s = 0.05$. The results are presented in Figure 9. The plots showing the slip velocity as a function of position and time indicate that the initiation time increases with increasing barrier width. As a matter of fact the initial weakening rate of the effective laws, also plotted on Figure 9, is decreasing with increasing barrier width. When the size of the barrier or equivalently the distance between the cracks is increasing, the interaction between the slipping patches diminishes and the collective instability behavior is delayed. On the other hand, the slip for which the change of weakening occurs is almost constant, as expected from the model of stress concentration on the strong patches.

9. Case of a Very Strong Heterogeneity

The case where $\delta\mu_s = 0.25$ corresponds to a very strong heterogeneity of the fault. The weak patches can begin to slip at relatively low stress (here $0.8S$) while large stress concentration are required to overcome the resistance of the barriers (here $1.05S$). As shown in Figure 8, it is difficult to identify directly an effective friction law from the stress-displacement relation obtained with the numerical solution of the complete model because of the perturbation by the very energetic waves produced by the rupture of the barriers. Following the simple two-phase interpretation presented in section 6, we define the friction law by a piecewise linear function. The initial slope defines the first segment between 0 and 0.094 m. A second segment is given by the linear weakening observed between 0.094 and 0.125 m. The friction is constant for larger slip. One must note here that the slip for which the friction becomes constant (the critical slip) is larger for the effective law than for the local laws on both the weak and strong patches. This important point will be discussed in the section 10. The comparison of slip velocity profiles obtained for the complete model and the homogeneous fault with the renormalized law is presented in Figure 10. With the complete heterogeneous model the solution exhibits strong peaks associated with the break of the asperities, which lead to the bump seen in Figure 8. On the contrary, the homogeneous effective model produces smooth profiles. Nevertheless, on average, the agreement between the two models is excellent. The effective model is not expected to reproduce the small-scale features of the heterogeneous model. The global features, that is, timing, average shape of the profiles, and mean value of slip

velocity at a given time, are well reproduced by the effective model.

10. Discussion and Conclusions

Faults are very far from idealized planes. They exhibit geometrical irregularities as well as variations in the elastic properties of the surrounding medium. These facts cannot be ignored when setting up simple friction models. In this context the significance of the friction law must be questioned. Our simple numerical experiments show that the apparent friction does not correspond to a local physical property of the surface. If we define an effective friction law at a given length scale, we find that it is widely determined by the heterogeneity of resistance at the first smaller scale. Indeed this effect is expected from scale to scale. It is natural for seismologists to consider the scale of the laboratory experiments as the one at which an intrinsic property of the sliding surface is measured. This typical length is the centimeter. The length of a fault segment for a large earthquake is of the order of tens of kilometers, that is 6 orders of magnitude larger than the laboatory scale. It is therefore not surprising that the properties of the faults at these different scales are completely different. The simple numerical experiments presented here show that the initial weakening rate decreases when moving from a small scale to a larger one in the presence of resistance heterogeneity. Since the initial weakening of a friction law determines the initiation duration, as discussed by *Ionescu and Campillo* [1999], the results presented here imply that the duration of the initiation is increasing with the scale of the event considered. More specifically, the initiation time associated with a large earthquake that develops on a large area of an heterogeneous fault cannot be compared with the time deduced from the friction laws measured in the laboratory. Indeed, the initiation time can be much larger for the large earthquake, by orders of magnitude.

The friction law for a seismogenic fault has been proposed from the analysis of records from the Landers earthquake by *Madariaga and Olsen* [2000] and S. Peyrat et al. (Dynamic Modeling of the 1992 Landers Earthquake, submitted to *Journal Geophysical Reserch*, 2000) in the form of a slip weakening law similar to the one used in our computations. They found the critical slip to be of the order of tens of centimenters while the value of the critical slip L_c is typically 1μm in dynamic laboratory experiment [*Ohnaka and Shen*, 1999]. Our results also indicate that the critical slip of the effective law is larger than those of the local laws imposed on the heterogeneous fault. Considering an homogeneous fault surface of unit area, one can define the fracture energy density as the energy in excess to the work done against the constant dynamic friction. It is proportional to the area between the friction law and the line $\mu = \mu_f$ in Figure 1: that is, $(\mu_s - \mu_d)L_c/2$. Physically, it corresponds to the energy spent in the irreversible processes

occurring during the weakening of the fault. In an heterogeneous fault as the one considered in our model, the total fracture energy can be computed by integrating over the whole fault. We have seen that the heterogeneous problem can be renormalized at a larger scale through the effective friction law. An important aspect of this modeling is to check the conservation of the fracture energy between the original heterogeneous model and its renormalized version. Numerically, we find an excellent agreement between fracture energies for models with weak perturbations of strength. To be more specific, when the critical slip of the effective law is equal to the one of the local law, we found an exact agreement. This corresponds to the cases of the models with static friction perturbation of 2% and 10%. On the other hand, there is not a match when considering a very strong heterogeneity, such as the model with strong barriers where the friction increase is 25%. Under these conditions the effective friction law implies a fracture energy much larger than that of the actual model. This can be understood easily. One can notice in Figure 10 that before the breaking of the strong barriers, the weak patches have already finished the initiation process and have entered locally into the phase of crack propagation. In other words, when the slip begins on the strong parts, the slip is already larger than the local critical slip on the weak parts. That is why the effective critical slip is larger than the local one. At the same time, the energy associated with the weakening in the effective model includes a part of the work done against the dynamic friction. In this particular case, the excess in fracture energy is 15%. This simple observation has important implications for practical analysis. The apparent critical slip L_c is much larger from earthquake studies (that are at a kilometric scale) than from laboratory experiments. We suggest that this difference is related to the strong heterogeneity of the properties of actual fault surfaces at every scale [see *Main*, 1996]. The larger L_c results from a process of successive renormalizations. In this case the apparent fracture energy, deduced from seismological analysis, is a crude overestimation of the actual fracture energy.

We showed how the small-scale heterogeneity of fault strength can be represented by an effective friction law which significantly differs from the local microscopic laws. The presence of barriers that slow down the growth of the instability is accounted for in the effective law by an initial weakening rate that is much smaller than that for the local laws. This initial weakening rate governs the time of initiation. This apparent weakening is dependent on the distribution of weak and strong parts of the fault. It can be computed directly from the largest positive eigenvalue of the spectral problem associated with the heterogeneous problem. Indeed, while slip is developing on the weak parts of the fault, stress concentrations build up on the barriers that eventually fail. At this point the system is changing drastically, even in its geometry. There is no possible linearization acceptable at this stage. Nevertheless, our dynamic computations shows that in the cases we considered, the system evolves very rapidly toward a new stable geometry where the entire fault is slipping. At that time, the effective friction exhibits a constant weakening rate that can be deduced from a spectral analysis.

We have only considered here one step in the change of scale. The fault length being the reference scale, we studied the effect of heterogenity of strength with a characteristic length 10 times smaller. We showed the accuracy of an effective friction law to describe the instability at the larger scale. Indeed, since we accurately know the friction law only at the laboratory scale, to set up a macroscopic law for use in modeling large earthquakes, one must perform a series of renormalizations taking into account the statistical properties of the fault heterogeneity.

References

Andrews, D.J., Rupture velocity of plane strain shear cracks, *J. Geophys. Res., 81*, 5679-5687, 1976.

Archuleta, R.J., A faulting model for the 1979 Imperial Valley earthquake, *J. Geophys. Res., 89*, 4559-4585, 1984.

Burridge, R., and L. Knopoff, Model and theoretical seismicity. *Bull. Seismol. Soc. Am., 57*, 341-371, 1967.

Campillo, M., and I.R. Ionescu, Initiation of an Antiplane Shear Instability under Slip Dependent Friction. *J. Geophys. Res., 102*, 20363-20371, 1997.

Carlson, J.M., and J.S. Langer, Model and theoretical seismicity, *Bull. Seismol. Soc. Am., 57*, 341-371, 1989.

Cotton, F., and M. Campillo, Frequency domain inversion of strong motions: Application to the 1992 earthquake, *J. Geophys. Res., 100*, 3961-3975, 1995.

Dascalu, C., I.R. Ionescu, and M. Campillo, Fault finiteness and initiation of dynamic shear instability, *Earth Planet. Sci. Lett., 177*, 163-176, 2000.

Dieterich, J.H., Modeling of rock friction, 1. Experimental results and constitutive equations. *J. Geophys. Res., 84*, 2161-2168, 1979.

Fukuyama, E., and R. Madariaga, Rupture dynamics of a planar fault in a 3D elastic medium: Rate- and slip-weakening friction, *Bull. Seismol. Soc. Am., 88*, 1-17, 1998.

Hartzell, S.H., and T.H. Heaton, Inversion of strong ground motion and teleseismic waveform data for the fault rupture history of the 1979 Imperial Valley, California, earthquake, *Bull. Seismol. Soc. Am., 73*, 1553-1583, 1983.

Ionescu, I.R. and M. Campillo, Numerical study of initiation: Influence of non-linearity and fault finiteness, *J. Geophys. Res., 104*, 3013-3024, 1999.

Madariaga R., Dynamics of an expanding circular crack, *Bull. Seismol. Soc. Am., 66*, 639-667, 1976.

Madariaga R., and K.B. Olsen, Criticality of rupture dynamics in three dimensions, *Pure Appl. Geophys.*, in press, 2000.

Main, I., Statistical physics, seismogenesis and seismic hazard, *Rev. Geophys., 34*, 4333-462, 1996.

Matsu'ura, M., H. Kataoka, and B. Shibazaki, Slip dependent friction law and nucleation processes in earthquake rupture, *Tectonophysics, 211*, 135-148, 1992.

Narteau, C., Shebalin, P., Holschneider M., Le Mouël J.L.,

and C.J. Allègre, Direct simulations of the stress redistribution in the scaling organization of fracture tectonics (S.O.F.T.) model, *Geophys. J. Int.*, in press, 2001.

Ohnaka M., and L. Shen, Scaling of the shear rupture process from nucleation to dynamic propagation: Implication of geometry irregularity of the rupturing surfaces, *J. Geophys. Res., 104*, 817-844, 1999.

Scholz, C.H., *The mechanics of Earthquakes and Faulting*, Cambridge Univ. Press, New York, 1990.

Umeda, Y., T. Yamashita, T. Tada, and N. Kame, Possible mechanisms of dynamic nucleation and arresting of shallow earthquakes faulting, *Tectonophysics, 261*, 179-192, 1996.

M. Campillo, Laboratoire de Géophysique Interne, Observatoire de Grenoble, Université Joseph Fourier, BP 53X, 38041 Grenoble Cedex, France, (Michel.Campillo@obs.ujf-grenoble)

P. Favreau, Institute for Crustal Studies, University of California, Santa Barbara, CA 93106, (pfavre@crustal.ucsb.edu)

I. R. Ionescu, Laboratoire de Mathématiques, Université de Savoie, 73376 Le Bourget-du-Lac Cedex, France, (Ioan.Ionescu@univ-savoie.fr)

C. Voisin, Department of Geological Sciences, San Diego State University, 5500 Campanile Drive, San Diego, CA 92182-1020. (cvoisin@moho.sdsu.edu)